Short-time scaling behavior of growing interfaces

Michael Krech
Fachbereich Physik, Bergische Universität Wuppertal, 42097 Wuppertal, Federal Republic of Germany

(Received 20 August 1996)

The short-time evolution of a growing interface is studied within the framework of the dynamic renormalization-group approach for the Kadar-Parisi-Zhang (KPZ) equation and for an idealized continuum model of molecular-beam epitaxy. The scaling behavior of response and correlation functions is reminiscent of the ''initial slip'' behavior found in purely dissipative critical relaxation (model A) and critical relaxation with conserved order parameter (model B), respectively. Unlike model A the initial slip exponent for the KPZ equation can be expressed by the dynamical exponent z. In 1+1 dimensions, for which z is known exactly, the analytical theory for the KPZ equation is confirmed by a Monte Carlo simulation of a simple ballistic deposition model. In 2+1 dimensions z is estimated from the short-time evolution of the correlation function. [S1063-651X(97)03001-8]

PACS number(s): 68.35 Fx, 64.60 Ht, 05.70 Ln, 05.40 +j

I. INTRODUCTION

Interface formation and growth are typical processes in nonequilibrium systems. From a technological point of view, two important examples are fluid flow in porous media (oil in rock) [1] and deposition of atoms during molecular-beam epitaxy (MBE) [1,2]. It is expected that at times much later than typical aggregation times and on macroscopic length scales these interfaces develop a characteristic scaling behavior, where the scaling exponents fall into certain dynamic *universality classes* [1–3] (see below). In certain cases, however, interfaces can also show turbulent, i.e., spatial, multiscaling behavior [4]. Usually a d-dimensional interface is embedded in $(d+1)$-dimensional space such that the interface position at time t can be described by a height function $h(\mathbf{x},t)$, where $\mathbf{x}$ denotes the lateral position in a d-dimensional reference plane given by, e.g., the surface of a substrate in MBE. Complete information about the scaling behavior is contained in the dynamic structure factor, which is related to the time displaced height-height correlation function $C(\mathbf{x}-\mathbf{x}',t,t')\equiv\langle h(\mathbf{x},t)h(\mathbf{x}',t')\rangle-\langle h(\mathbf{x},t)\rangle\langle h(\mathbf{x}',t')\rangle$, where a laterally translational invariant system is assumed. For $t,t'\to\infty$, and finite $|t-t'|$ the correlation function displays the asymptotic scaling behavior

$$C(\mathbf{x}-\mathbf{x}',t,t')=|\mathbf{x}-\mathbf{x}'|^{2\alpha}F_C(|t-t'|/|\mathbf{x}-\mathbf{x}'|^z), \quad (1.1)$$

where α denotes the *roughness* exponent and z is the *dynamic* exponent [1,2]. For a laterally translational invariant system the interfacial width $w^2(t)\equiv\langle h^2(\mathbf{x},t)\rangle-\langle h(\mathbf{x},t)\rangle^2$ is only a function of t and displays the scaling behavior $w(t)\sim t^\beta$ for late times, where $\beta=\alpha/z$ is the *growth* exponent. For MBE, as an example the scaling behavior displayed in Eq. (1.1) gives access to the exponents α and z both experimentally by reflection high-energy electron diffraction (see, e.g., Chap. 16 of Ref. [1]) and theoretically by continuum models [1,2] and Monte Carlo simulations [2,5]. Since the advent of the scanning tunneling microscope direct imaging techniques for interfaces have also become an important experimental tool [6].

Continuum descriptions of interfacial growth processes can be obtained from general symmetry principles and conservation laws obeyed by the growth process [1]. The resulting coarse-grained growth model is given by an evolution equation for $h(\mathbf{x},t)$ that has the form of a Langevin equation with Gaussian distributed noise. This has been done in Ref. [7] for the sedimentation of granular material and leads to the well known Edwards-Wilkinson (EW) equation. It is given by

$$\frac{\partial}{\partial t}h(\mathbf{x},t)=\nu\nabla^2 h(\mathbf{x},t)+\eta(\mathbf{x},t), \quad (1.2)$$

where the noise $\eta(\mathbf{x},t)$ has a Gaussian distribution with $\langle\eta(\mathbf{x},t)\rangle=0$ and

$$\langle\eta(\mathbf{x},t)\eta(\mathbf{x}',t')\rangle=2D\,\delta(\mathbf{x}-\mathbf{x}')\,\delta(t-t'). \quad (1.3)$$

The parameters ν and D are assumed to be constants and averages $\langle\ \rangle$ are taken over the noise distribution. From explicit solutions of Eq. (1.2) the exponents z and α are known exactly in any dimension d of the interface:

$$z=2, \quad \alpha=(2-d)/2. \quad (1.4)$$

Note that $d=2$ is the critical dimension of Eq. (1.2). One has $\alpha<0$ for $d>2$ so that the height-height correlation function $C(\mathbf{x}-\mathbf{x}',t,t')$ according to Eq. (1.1) *decays* with increasing distance $|\mathbf{x}-\mathbf{x}'|$. In $d=2$ $(\alpha=0)$ the correlations increase logarithmically.

The simplest possible nonlinear extension to the EW equation was considered systematically in Ref. [8]. The resulting Langevin equation, usually denoted as the Kadar-Parisi-Zhang (KPZ) equation, is given by

$$\frac{\partial}{\partial t}h(\mathbf{x},t)=\nu\nabla^2 h(\mathbf{x},t)+\frac{\lambda}{2}[\nabla h(\mathbf{x},t)]^2+\eta(\mathbf{x},t), \quad (1.5)$$

with Gaussian distributed noise according to Eq. (1.3). The additional parameter λ is again assumed to be a constant. In the long-time limit Eq. (1.5) has a global symmetry that is commonly denoted as Galileian invariance. This invariance originates from the equivalence of Eq. (1.5) to the Burgers equation for a vorticity-free velocity field $\mathbf{v}(\mathbf{x},t)=-\nabla h(\mathbf{x},t)$ and can be stated as follows. If $h(\mathbf{x},t)$ solves Eq. (1.5) for some noise function $\eta(\mathbf{x},t)$ then

$$h'(\mathbf{x},t)=h(\mathbf{x}-\mathbf{w}t,t)-\frac{1}{\lambda}\mathbf{w}\cdot\mathbf{x}+\frac{1}{2\lambda}\mathbf{w}^2t \tag{1.6}$$

is a solution of Eq. (1.5) for the noise function $\eta'(\mathbf{x},t)=\eta(\mathbf{x}-\mathbf{w}t,t)$ and any constant vector $\mathbf{w}$. An important consequence is that the exponents z and α of the KPZ equation fulfill the exact scaling relation [9,10]

$$\alpha+z=2. \tag{1.7}$$

Note that in $d=2$ the EW exponents also obey Eq. (1.7). The exponents of the KPZ equation are exactly known only in $d=1$, where

$$z=3/2, \quad \alpha=1/2 \tag{1.8}$$

due to the existence of a dissipation-fluctuation theorem [9,11]. In $d=2$ numerical investigations indicate $z\simeq1.6$ and $\alpha\simeq0.4$ [1]. For $d>2$ the asymptotic scaling behavior is governed either by the EW exponents [see Eq. (1.4), weak-coupling regime] or by another set of exponents inaccessible by analytical methods (strong-coupling regime) depending on the value of the effective coupling constant $g\equiv D\lambda^2/(4\nu^3)$ [1,9,10]. In $d=3$ numerical evidence suggests $z\simeq1.7$ and $\alpha\simeq0.3$ in the strong-coupling regime [1], still indicating rough interfaces in contrast to the EW scaling behavior in $d=3$ [see Eq. (1.4)]. Furthermore, it is interesting to note that the nonlinearity in Eq. (1.5) is the most relevant one, i.e., if present it renders all other nonlinearities irrelevant in the renormalization-group sense in the long-time limit. For intermediate times, however, the presence of other nonlinearities in the Langevin equation gives rise to various crossover phenomena [1,12]. The EW equation and the KPZ equation for $\lambda\neq0$ thus represent two different universality classes for interfacial growth. For $\lambda<0$ Eq. (1.5) can be viewed as a model for interface *corrosion* rather than growth [8].

With special regard to MBE growth it is worth noting that the requirement of mass conservation in ideal MBE [13] explicitly excludes the KPZ nonlinearity from a corresponding coarse-grained continuum theory. A simple Langevin equation for ideal MBE has been proposed in Ref. [13] (see also Refs. [14,15]):

$$\frac{\partial}{\partial t}h(\mathbf{x},t)=-\nu_1\nabla^4h(\mathbf{x},t)+\lambda_1\nabla^2[\nabla h(\mathbf{x},t)]^2+\eta(\mathbf{x},t), \tag{1.9}$$

where $\eta(\mathbf{x},t)$ is chosen according to Eq. (1.3). Mass conservation in combination with Eq. (1.3) immediately leads to the exact scaling relation $2\alpha-z+d=0$ for Eq. (1.9). Furthermore, a global symmetry analogous to Eq. (1.6), which can be written in the operator form [16]

$$\mathbf{x}\rightarrow\mathbf{x}-2\mathbf{w}t\nabla^2, \quad h\rightarrow h-\frac{1}{\lambda_1}\mathbf{w}\cdot\mathbf{x} \tag{1.10}$$

for any infinitesimal vector $\mathbf{w}$, yields the second exact scaling relation $\alpha+z=4$ [13,16]. The exponents z and α for ideal MBE are therefore known exactly in any dimension of physical interest:

$$z=(8+d)/3, \quad \alpha=(4-d)/3, \tag{1.11}$$

indicating $d=4$ as the critical dimension of Eq. (1.9).

In this paper Eqs. (1.5) and (1.9) are used as paradigms for continuum descriptions of interfacial growth processes. In linear theory (i.e., $\lambda=\lambda_1=0$) their dynamical exponents are given by $z=2$ and $z=4$ [see Eqs. (1.4) and (A13)], respectively, and therefore Eqs. (1.5) and (1.9) may be viewed as nonequilibrium analogs of the dynamical models A and B for critical relaxation, respectively. In order to invesitgate the scaling behavior of, e.g., $C(\mathbf{x}-\mathbf{x}',t,t')$ for $t'\ll t$ the initial condition $h(\mathbf{x},t=0)=0$ motivated by deposition processes is used simultaneously with Eqs. (1.5) and (1.3) or Eqs. (1.9) and (1.3), respectively. Perturbative and nonperturbative aspects of short-time scaling for the two models are discussed in Secs. II and III within the framework of dynamic renormalization [17–19]. Numerical results from ballistic deposition are presented in Sec. IV and a summary of the main results is given in Sec. V.

II. KPZ EQUATION

Due to the spatial translational invariance of the deposition processes studied here calculations are most conveniently performed in Fourier space. With the definition $h(\mathbf{x},t)=(2\pi)^{-d}\int d^dq\exp(i\mathbf{q}\cdot\mathbf{x})h(\mathbf{q},t)$ for the Fourier transform the dynamic functional $\mathcal{J}[\tilde{h},h]$ for the KPZ equation [9,17,20] can be written as the sum of the Gaussian part

$$\mathcal{J}_0[\tilde{h},h]=\int\frac{d^dq}{(2\pi)^d}\int_0^\infty dt\bigg\{D\tilde{h}(\mathbf{q},t)\tilde{h}(-\mathbf{q},t)-\tilde{h}(\mathbf{q},t)\times\left(\frac{\partial}{\partial t}h(-\mathbf{q},t)+\nu\mathbf{q}^2h(-\mathbf{q},t)\right)\bigg\} \tag{2.1}$$

and the interaction part

$$\mathcal{J}_1[\tilde{h},h]=-\frac{\lambda}{2}\int\frac{d^dq_1}{(2\pi)^d}\int\frac{d^dq_2}{(2\pi)^d}\int_0^\infty dt\,\mathbf{q}_1\cdot\mathbf{q}_2\times\tilde{h}(-\mathbf{q}_1-\mathbf{q}_2,t)h(\mathbf{q}_1,t)h(\mathbf{q}_2,t), \tag{2.2}$$

where $\tilde{h}(\mathbf{q},t)$ is the Fourier transform of the response field [18]. The initial condition $h(\mathbf{q},0)=0$, which is implicitly assumed in Eqs. (2.1) and (2.2), breaks the temporal translational invariance of the KPZ dynamics. In a more general form this broken symmetry can be expressed in terms of an additional contribution to $\mathcal{J}_0$ that is localized at the time "surface" $t=0$:

$$\mathcal{J}_s[h]=\frac{c}{2}\int\frac{d^dq}{(2\pi)^d}[h(\mathbf{q},0)-h_0(\mathbf{q})]^2. \tag{2.3}$$

From the analogy of Eq. (2.3) with surface contributions to the Ginzburg Landau functional in the theory of static surface critical phenomena [21] and dimensional arguments the only possible fixed point values of c under the renormalzation group are $c=\pm\infty$ and $c=0$. In the latter case additive renormalizations of c are supposed to be absorbed in c itself, which can be accomplished by the dimensional regularization scheme. On the other hand, Eq. (2.3) generates a distribution function $\exp(-\mathcal{J}_s[h])$ of initial configurations $h(\mathbf{q},0)$ of the deposition field that leaves the fixed-point value $c=\infty$ as the only choice due to the requirement of normalizability of distribution functions. Deviations of c from this fixed-point value therefore generate only corrections to scaling [17,21], which will be disregarded here. From Eq. (2.3) one then has the initial condition $h(\mathbf{q},0)=h_0(\mathbf{q})$. As shown in Appendix A, $h_0(\mathbf{q})$ can be incorporated into a source contribution to the dynamic functional [see Eqs. (A3) and (A6)] and therefore we stick to $h_0(\mathbf{q})=0$ in the following. The correlation and the response propagator are now easily derived from Eq. (2.1). The results are summarized in Appendix A.

The introduction of an initial condition, striktly speaking, also breaks Galileian invariance [see Eq. (1.6)]. If one demands $h(\mathbf{x},0)=0$ as the initial condition for h then $h'(\mathbf{x},t)$ solves Eq. (1.5) with the new initial condition $h'(\mathbf{x},0)=-\mathbf{w}\cdot\mathbf{x}/\lambda$. However, as indicated above, one only has to transform the source fields accordingly in order to restore the old initial condition. Therefore the Galilei transformation [see Eqs. (1.6), (A3), and (A6)]

$$
\begin{aligned}
h'(\mathbf{q},t)&=e^{-i\mathbf{q}\cdot\mathbf{w}t}h(\mathbf{q},t)-(2\pi)^d\frac{i}{\lambda}\mathbf{w}\cdot\frac{\partial}{\partial\mathbf{q}}\delta(\mathbf{q}),\\
\tilde{h}'(\mathbf{q},t)&=e^{-i\mathbf{q}\cdot\mathbf{w}t}\tilde{h}(\mathbf{q},t),\\
j'(\mathbf{q},t)&=e^{-i\mathbf{q}\cdot\mathbf{w}t}j(\mathbf{q},t),\\
\tilde{j}'(\mathbf{q},t)&=e^{-i\mathbf{q}\cdot\mathbf{w}t}\tilde{j}(\mathbf{q},t)+(2\pi)^d\frac{i}{\lambda}\mathbf{w}\cdot\frac{\partial}{\partial\mathbf{q}}\delta(\mathbf{q})\,\delta(t)
\end{aligned}
\tag{2.4}
$$

restores the Galileian invariance of the generating functional so that the corresponding Ward identities (see Ref. [9]) remain valid. Note that Eq. (2.4) should be read as an infinitesimal transformation, i.e., terms of order $\mathbf{w}^2$ have been neglected.

The renormalization-group treatment of Eq. (1.5) can now be set up following standard procedures [8,9,20]. For the case at hand it is most convenient to combine the dimensional regularization scheme for the KPZ equation [9] with the treatment of the short-time singularites documented in Ref. [17]. One defines the effective coupling constant

$$g\equiv D\lambda^2/(4\nu^3) \tag{2.5}$$

and the renormalized parameters ν^R, D^R, and u [8,9,20],

$$\nu^R\equiv Z_\nu\nu,\ \ D^R\equiv Z_D D,\ \ u\equiv Z_g g\mu^{\varepsilon}/[2^{d-1}\pi^{d/2}(2-d/2)], \tag{2.6}$$

where $\varepsilon=d-2$ and μ is an arbitrary momentum scale that absorbs the naive dimension of g [see Eq. (2.5)]. One finds the renomalization factors [9,20] (see also Appendix C)

$$
\begin{aligned}
&Z_\nu=1+\frac{d-2}{d}\frac{u}{\varepsilon}+O(u^2),\quad Z_D=1-\frac{u}{\varepsilon}+O(u^2),\\
&Z_h=\tilde{Z}_h=1\,,\quad Z_g=Z_D Z_\nu^{-3}\,,
\end{aligned}
\tag{2.7}
$$

where the $1/\varepsilon$ poles indicate the presence of ultraviolet singularities [9]. The nonrenormalization of h and $\tilde{h}$ indicated in Eq. (2.7) is *exact* and a consequence of Eq. (B1) (see Appendix B). The relation $Z_g=Z_D Z_\nu^{-3}$ which is equivalent to $\lambda^R=\lambda$, is a consequence of Galileian invariance in the long-time limit [see Eq. (1.6) and Refs. [8,9,20]] and therefore also holds to all orders in perturbation theory. The renormalization-group flow at late times is then governed by the Wilson functions [9,20]

$$
\begin{aligned}
&\zeta_\nu(u)=\frac{d-2}{d}u+O(u^2),\quad \zeta_D(u)=-u+\mathcal{O}(u^2),\\
&\beta(u)=[d-2+\zeta_D(u)-3\zeta_\nu(u)]u,
\end{aligned}
\tag{2.8}
$$

where the relation between $\beta(u)$, $\zeta_D(u)$, and $\zeta_\nu(u)$ is again *exact*. The higher-order corrections to ζ_ν and ζ_D indicated in Eq. (2.8) vanish in $d=1$ due to the existence of a fluctuation-dissipation theorem [9,11]. The fluctuation-dissipation theorem also requires $Z_\nu=Z_D$ in $d=1$ so that $\zeta_\nu(u)=\zeta_D(u)$ and $\nu/D=\nu^R/D^R$ [see Eqs. (2.6) and (2.7)]. We also want to emphasize here that $\zeta_\nu(u)$ and $\zeta_D(u)$ as given by Eq. (2.8), like any other finite-order perturbation theory, do not give access to the strong-coupling regime of Eq. (1.5) for $d\geqslant 2$.

In analogy with critical phenomena in semi-infinite geometries [21] modifications of the scaling behavior of response and correlation functions must be expected in the ''time surface'' $t=0$ [17]. In order to determine the corresponding anomalous short-time scaling dimensions of response and correlation functions we introduce two renormalization factors Z_0 and $\tilde{Z}_0$ by the renormalization prescription (see also Ref. [17])

$$h(\mathbf{q},0)=Z_0^{1/2}h^R(\mathbf{q},0),\quad \tilde{h}(\mathbf{q},0)=\tilde{Z}_0^{1/2}\tilde{h}^R(\mathbf{q},0). \tag{2.9}$$

These Z factors are determined by Eq. (B1) and the operator identity

$$\frac{\partial}{\partial t}h(\mathbf{q},t=0)=2D\tilde{h}(\mathbf{q},t=0) \tag{2.10}$$

derived in Appendix B. For the weak-coupling regime of the KPZ equation $(d=1)$ the perturbative analysis of Appendix B consitutes a rigorous proof of Eq. (2.10) and the relations that follow from it (see below). In the strong-coupling regime $(d\geqslant 2)$, however, the corresponding perturbative analysis no longer provides a rigorous proof of Eq. (2.10), because relations that are valid order by order in perturbation theory may be violated at a strong-coupling fixed point (see Appendix B). This has to be kept in mind for the following considerations, although the perturbative result can be regarded as evidence in favor of the general validity of Eq. (2.10).

From Eq. (B1) for $t'=0$ we immediately find the exact identity $\tilde{Z}_0=1$. Insertion of Eqs. (2.6) and (2.9) into Eq. (2.10) leads to the second exact identity $Z_0=Z_D^{-2}\tilde{Z}_0$, which determines Z_0 in terms of the known Z factor Z_D [see Eq. (2.7)]. These identities translate into the *exact* relations

$$\tilde{\zeta}_0(u)=0, \quad \zeta_0(u)=-2\zeta_D(u) \tag{2.11}$$

among the corresponding Wilson functions [see also Eq. (2.8)]. From Eq. (2.11) one concludes that (i) the response function $G(\mathbf{q},t,t')$ does not exhibit an anomalous scaling dimension in the short-time limit $t'\to 0$ (i.e., $t'\ll t$) and (ii) the anomalous short-time exponent of the correlation function $C_0(\mathbf{q},t,t')$ can be expressed by long-time exponents [see Eq. (1.8) and the following text]. These properties set KPZ short-time dynamics markedly apart from model A.

In order to determine the short-time scaling exponent of $C(\mathbf{q},t,t'\ll t)$ we employ the ''short-distance expansion'' [17] $h(\mathbf{q},t'\to 0)=\sigma(t')(\partial/\partial t')h(\mathbf{q},t'=0)+\cdots$ inside the correlation function C, which means that

$$C(\mathbf{q},t,t'\ll t)=\sigma(t')\frac{\partial}{\partial t'}C(\mathbf{q},t,t'=0)+\cdots. \tag{2.12}$$

Employing the renormalization prescriptions given by Eqs. (2.6) and (2.9), one finds

$$\begin{gathered}\sigma(t')=Z_0^{-1/2}\sigma^R(\mu,t',u),\\ \frac{\partial}{\partial t'}C(\mathbf{q},t,t'=0)=Z_0^{1/2}\frac{\partial}{\partial t'}C^R(\mu,\mathbf{q},t,t'=0,u)\end{gathered} \tag{2.13}$$

for the corresponding renormalized short-distance expansion [see Eq. (2.12)]. Using dimensional analysis, the renormalized functions defined by Eq. (2.13) can be written in the scaling form

$$\sigma^R(\mu,t',u)=t'f(y',u) \quad \text{with} \quad y'=\nu(\mu)\mu^2t', \tag{2.14}$$

$$\frac{\partial}{\partial t'}C^R(\mu,\mathbf{q},t,t'=0,u)=D(\mu)g(x,y,u) \quad \text{with} \quad x=\mathbf{q}/\mu,$$

$$y=\nu(\mu)\mu^2t,$$

where μ has been chosen as the renormalization-group flow parameter. It is now straightforward to derive the renormalization-group equations for the *dimensionless* scaling functions $f(y',u)$ and $g(x,y,u)$ defined by Eq. (2.14). Using Eqs. (2.6) and (2.9) one obtains

$$\left[[2+\zeta_\nu(u)]y'\frac{\partial}{\partial y'}+\beta(u)\frac{\partial}{\partial u}-\frac{\zeta_0(u)}{2}\right]f(y',u)=0, \tag{2.15}$$

$$\left[-x\frac{\partial}{\partial x}+(2+\zeta_\nu(u))y'\frac{\partial}{\partial y'}+\beta(u)\frac{\partial}{\partial u}+\zeta_D(u)\right.$$
$$\left.+\frac{\zeta_0(u)}{2}\right]g(x,y,u)=0.$$

At the infrared stable renormalization-group fixed point $u=u^*$ Eq. (2.15) has the solutions

$$f(y',u^*)=y'^{\eta_0/2z}, \quad g(x,y,u^*)=y^{-(2\eta_D+\eta_0)/2z}g'(x^zy), \tag{2.16}$$

where $\eta_a=\zeta_a(u^*)$ for $a=\nu,D,0$; $z=2+\eta_\nu$; and g' is a scaling function left undetermined by Eq. (2.15). Combining Eqs. (2.12), (2.14), and (2.16) one finds after a few manipulations

$$C(\mathbf{q},t,t'\ll t)=(t'/t)^{1+\eta_0/2z}|\mathbf{q}|^{\eta_D-z}f_C(|\mathbf{q}|^zt) \tag{2.17}$$

for the short-time scaling behavior of the correlation function. For $u^*=0$ one obtains the EW scaling exponents [see Eq. (1.4)] and $\eta_0=0$ in Eq. (2.17). For any *nonzero* fixed point u^* the exact scaling relation $\eta_D=3z-4-d$ holds [see Eq. (2.8)], which is equivalent to Eq. (1.7). From Eq. (2.11) one finally obtains for the short-time exponent [see Eq. (2.17)]

$$1+\eta_0/2z\equiv\theta=1-\eta_D/z=(d+4)/z-2. \tag{2.18}$$

In $d=1$ the exact value $\theta=4/3$ can be obtained from Eq. (1.8). From numerical estimates for z in $d=2$ and $d=3$ (see Sec. I) one obtains $\theta\simeq 1.7$ and $\theta\simeq 2.1$, respectively. The exponent relation given by Eq. (2.18) simply means that the short-time and the long-time scaling behavior of the correlation function are *identical*, i.e., the short-time scaling behavior can be obtained by extrapolating the t' dependence of $C(\mathbf{q},t,t')$ from $t'\sim t$ to $t'=0$. In fact, the scaling relation given by Eq. (2.18) can be derived independently by analyzing the fluctuation spectrum of the interface displacement velocity averaged over a macroscopic portion of the interfacial area [22].

Finally, we remark that some alternative scaling forms for C can be obtained from the definition of the growth exponent $\beta=\alpha/z$, which leads to $\theta=d/z+2\beta$. The scaling behavior displayed in Eq. (2.17) can then be written in the simplified form $C(\mathbf{q},t,t'\ll t)=t'^{\theta}g_C(|\mathbf{q}|^zt)$, where $g_C(y)=y^{-\theta}f_C(y)$. In real space the correlation function has the scaling form $C(\mathbf{x},t,t'\ll t)=(t'/t)^{\theta}|\mathbf{x}|^{2\alpha}G_C(t/|\mathbf{x}|^z)$.

The absence of anomalous scaling exponents for $G(\mathbf{q},t,t')$ for $t'\ll t$ does not neccessarily mean that G is *analytic* for $t'\to 0$. Exponents describing the asymptotic short-time behavior are in general functions of the dimensionality d and therefore may take noninteger values for certain d. Similar considerations apply to the crossover behavior of G for $t\to\infty$ with *fixed* $t-t'$. For details we refer to Appendix C, where some results from perturbation theory are discussed in the case $d=1$.

III. IDEAL MBE

In terms the deposition field $h(\mathbf{q},t)$ and the response field $\tilde{h}(\mathbf{q},t)$ the dynamic functional $\mathcal{J}[\tilde{h},h]$ for Eq. (1.9) [2,13,14] is also written as the sum of the Gaussian part

$$\mathcal{J}_0[\tilde{h},h]=\int\frac{d^dq}{(2\pi)^d}\int_0^\infty dt\left\{D\tilde{h}(\mathbf{q},t)\tilde{h}(-\mathbf{q},t)-\tilde{h}(\mathbf{q},t)\right.$$
$$\left.\times\left(\frac{\partial}{\partial t}h(-\mathbf{q},t)+\nu_1(\mathbf{q}^2)^2h(-\mathbf{q},t)\right)\right\} \tag{3.1}$$

and the interaction part

$$\mathcal{J}_1[\tilde{h},h]=\lambda_1\int\frac{d^dq_1}{(2\pi)^d}\int\frac{d^dq_2}{(2\pi)^d}\int_0^\infty dt(\mathbf{q}_1+\mathbf{q}_2)^2\mathbf{q}_1\cdot\mathbf{q}_2 \times\tilde{h}(-\mathbf{q}_1-\mathbf{q}_2,t)h(\mathbf{q}_1,t)h(\mathbf{q}_2,t), \quad (3.2)$$

where the initial condition $h(\mathbf{q},0)=0$ is again implicitly assumed in Eqs. (3.1) and (3.2). As described in Sec. II and Appendix A this special initial condition is sufficient to study the short-time scaling behavior of response and correlation functions for ideal MBE. The results of Gaussian theory as implied by Eq. (3.1) are summarized in Appendix A.

The further analysis of Eq. (1.9) can be carried out along the lines of the analysis of the KPZ equation presented in Sec. II. First, we note that the invariance under the infinitesimal transformation given by Eq. (1.10) in the presence of the initial condition $h(\mathbf{q},0)=0$ is restored by the transformation

$$\begin{aligned}
h'(\mathbf{q},t)&=e^{2iq^2\mathbf{q}\cdot\mathbf{w}t}h(\mathbf{q},t)-(2\pi)^d\frac{i}{\lambda_1}\mathbf{w}\cdot\frac{\partial}{\partial\mathbf{q}}\delta(\mathbf{q}),\\
\tilde{h}'(\mathbf{q},t)&=e^{2iq^2\mathbf{q}\cdot\mathbf{w}t}\tilde{h}(\mathbf{q},t),\\
j'(\mathbf{q},t)&=e^{2iq^2\mathbf{q}\cdot\mathbf{w}t}j(\mathbf{q},t),\\
\tilde{j}'(\mathbf{q},t)&=e^{2iq^2\mathbf{q}\cdot\mathbf{w}t}\tilde{j}(\mathbf{q},t)+(2\pi)^d\frac{i}{\lambda_1}\mathbf{w}\cdot\frac{\partial}{\partial\mathbf{q}}\delta(\mathbf{q})\delta(t),
\end{aligned}\quad (3.3)$$

where terms of the order $\mathbf{w}^2$ have been neglected. In analogy with the Galileian invariance of Eq. (1.5), this symmetry leads to the nonrenormalization of the nonlinearity: $\lambda_1^R=\lambda_1$ [see also Eq. (2.7) and Refs. [13,16]]. Second, Eq. (1.9) has the global symmetry of mass conservation, which in contrast to Eq. (2.6) leads to the *additional* nonrenormalization of the noise correlation amplitude [see Eq. (1.3)]: $D^R=D$ [13,16]. If one defines an effective coupling constant by [13]

$$g_1\equiv D\lambda_1^2/\nu_1^3 \quad (3.4)$$

and the renormalized parameters ν_1^R, D^R, and u,

$$\nu_1^R\equiv Z_{\nu_1}\nu_1,\quad D^R\equiv Z_D D,\quad u\equiv\frac{Z_{g_1}g_1\mu^\varepsilon}{2^{d-1}\pi^{d/2}(2-d/4)}\frac{\Gamma(d/4)}{\Gamma(d/2)}, \quad (3.5)$$

where $\varepsilon=d-4$ and μ is an arbitrary momentum scale that absorbs the naive dimension of g_1 [see Eq. (3.4)] then the renomalization-group results for Eq. (1.9) in the long-time limit can be summarized as (see also Appendix C)

$$Z_{\nu_1}=1+\frac{d-6}{d}\frac{u}{\varepsilon}+O(u^2),\quad Z_D=1,$$

$$Z_h=\tilde{Z}_h=1,\quad Z_g=Z_{\nu_1}^{-3}. \quad (3.6)$$

The $1/\varepsilon$ poles indicate the presence of ultraviolet singularities and the nonrenormalization of h and $\tilde{h}$ indicated in Eq. (3.6) is again a consequence of Eq. (B1). The corresponding renormalization-group flow is therefore governed by only two nontrivial Wilson functions, namely,

$$\zeta_{\nu_1}(u)=\frac{d-6}{d}u+O(u^2),\quad \beta(u)=[d-4-3\zeta_{\nu_1}(u)]u, \quad (3.7)$$

where the relation between $\beta(u)$ and $\zeta_{\nu_1}(u)$ is *exact* [see Eq. (3.6)]. For any infrared stable fixed point $u^*\neq 0$ Eq. (3.7) yields $\zeta_{\nu_1}(u^*)\equiv\eta_{\nu_1}=(d-4)/3$, from which the exponents given by Eq. (1.11) follow directly.

In order to investigate the short-time behavior of the response and the correlation function of Eq. (1.9) short-time renormalization factors Z_0 and $\tilde{Z}_0$ are defined as in Eq. (2.9). From Eqs. (B1) and (2.10), which also hold for Eq. (1.9) (see Appendix B), one immediately obtains $\tilde{Z}_0=1$ and $Z_0=Z_D^{-2}\tilde{Z}_0=1$, where Eq. (3.6) has been used. We thus conclude that in contrast to KPZ dynamics for ideal MBE *neither* the response function $G(\mathbf{q},t,t')$ *nor* the correlation function $C(\mathbf{q},t,t')$ exhibit anomalous scaling behavior for $t'\ll t$, which is reminiscent of the short-time behavior of model B in critical relaxation [17]. Finally, we note that in contrast to model B the noise in Eq. (1.9) is *not conserved* [see Eq. (1.3)]. Equation (1.9) with purely *conserved* noise has been considered in Ref. [16] (see also Ref. [1]). The qualitative short-time behavior is the same as that described here. However, with special regard to MBE, the case of purely conserved noise does not play the same central role as Eq. (1.9) with nonconserved noise [2] and we therefore refrain from discussing any details here.

Concerning the asymptotic short-time behavior of $G(\mathbf{q},t,t')$ and $C(\mathbf{q},t,t')$ and the crossover to their asymptotic long-time behavior one finds properties that are similar to the KPZ behavior mentioned in Sec. II. Some details obtained from perturbation theory are reported in Appendix C.

IV. BALLISTIC DEPOSITION

The scaling behavior of $C(\mathbf{q},t,t'\ll t)$ according to Eq. (2.17) can be tested numerically by a Monte Carlo simulation of a simple ballistic deposition model on a lattice with periodic boundary conditions [1]. For convenience we restrict ourselves to $d=1$ here. The continuum description used in Secs. II and III is replaced by a discretized description according to

$$h(x,t)=h(x=aj,t=n/(FL))\equiv ah_j(n), \quad (4.1)$$

where the lattice constant a is assumed to be the same both *in* the plane of the substrate and perpendicular to it. The lattice has L sites, F is the incoming particle flux, and n is the number of deposited particles. Furthermore, the incoming particle flux F has been normalized to unity, so that t in Eq. (4.1) is dimensionless and given by the number of deposited layers. Finally, $h_j(n)$ defined by Eq. (4.1) is also dimensionless and denotes the number of particles deposited at lattice site j after n particles have been deposited on the lattice. Ballistic deposition on a one-dimensional substrate is defined by the *deterministic* growth rule

$$h_j(n+1)=\max[h_{j-1}(n),h_j(n)+1,h_{j+1}(n)] \quad (4.2)$$

(see, e.g., Ref. [1]), where the site j in Eq. (4.2) has been selected randomly from the L sites of the lattice. For periodic boundary conditions $h_1(n)$ and $h_L(n)$ are treated as nearest neighbors in Eq. (4.2).

In order to measure the scaling behavior of $C(\mathbf{q},t,t')$ given by Eq. (2.17) for the above discrete model a discrete Fourier transform is defined by

$$\hat{h}_q(n)=\frac{1}{L}\sum_{j=1}^{L} h_j(n)e^{-iqaj} \quad \text{with} \quad q=\frac{2\pi}{L}m, \tag{4.3}$$

where m is an integer and $0\leq m\leq L-1$. Using Eq. (4.3) we define the discrete version of the height-height correlation function in Fourier space by

$$C_L(q,t,t')=\langle[\hat{h}_q(n)-\langle\hat{h}_q(n)\rangle][\hat{h}_q(n')-\langle\hat{h}_q(n')\rangle]\rangle,$$
$$n=FLt, \quad n'=FLt', \tag{4.4}$$

where the angular brackets denote an average over different realizations of the deposition process and the time arguments t and t' are reintroduced for convenience. For the measurement of the short-time exponent θ [see Eq. (2.18)] it is sufficient to measure $C_L(q,t,t')$ for $q=0$. In this case Eq. (4.4) defines the time displaced correlation function of the spatially averaged deposition height $\hat{h}_{q=0}(n)$, which can be measured very quickly during the simulation. In practice a measurement is done after the deposition of one layer, i.e., the time step is $\Delta t=1$.

Like a real deposition process, the simulation is characterized by an *a priori* unknown microscopic aggregation time t_a. A scaling behavior of C_L according to Eq. (2.17) can only be observed for $t'\gg t_a$. On the other hand, $t'\ll t$ is required for Eq. (2.17) to hold, so that short-time scaling is restricted to the time window $t_a\ll t'\ll t$. Furthermore, the lattice size L must be chosen sufficiently large in order to avoid the onset of finite-size crossover effects if $t'^{1/z}\sim L$ when t' is still much smaller than t. For the simulation described here $t=2000$ and $L\geq 480$ fulfill the above requirements. In order to cope with the very small signal-to-noise ratio in each measurement of $C_L(0,t,t')$ for $t'\ll t$ averages are taken over 10^5 realizations. These are distributed over 40 individual runs at every point in time for all lattice sizes. The result is displayed in Fig. 1, where $C_L(0,t,t')$ is shown as a function of t'/t for fixed $t=2000$ and for $L=480$, 960, and 1920. For clarity the statistical error is shown only at a few points in time. As can be seen from Fig. 1, there is slightly more than one decade in t'/t available to determine the short-time exponent θ. Using the least-squares method in the interval $0.03\leq t'/t\leq 0.4$, one finds

$$\theta=1.349\pm 0.005 \tag{4.5}$$

for $L=1920$ as the best estimate for θ from the data shown in Fig. 1. Although the agreement with the theoretical value $\theta=4/3$ is very good, there is still a systematic deviation well outside the statistical error, which is one standard deviation in Eq. (4.5). One source of systematic errors is the finite lattice size. For example, one finds $\theta=1.37$ for $L=480$ and for $L=240$ (not shown in Fig. 1) one even has $\theta=1.40$, which indicates that finite lattice corrections to Eq. (2.17) are

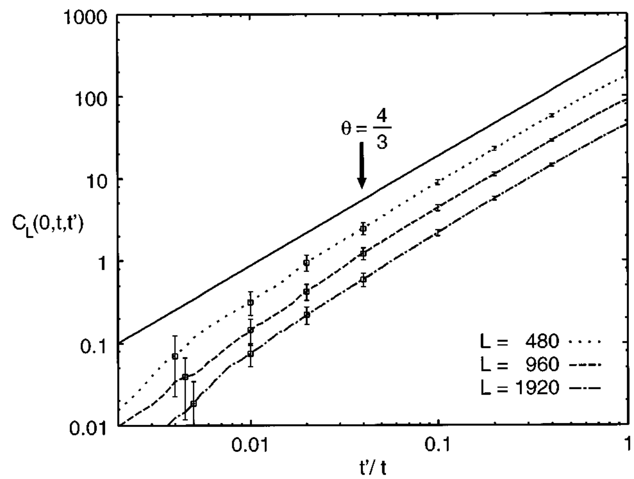

FIG. 1. Correlation function $C_L(\mathbf{0},t,t')$ in $d=1$ as a function of t'/t for $0.002\leq t'/t\leq 1$ and $L=480$ (dotted line), $L=960$ (dashed line), and $L=1920$ (dash-dotted line). The error bars are shown only at a few selected points in time and represent one standard deviation. The solid line displays a power law with the theoretical short-time exponent $\theta=4/3$. The data follow this power law rather accurately in the interval $0.03\leq t'/t\leq 0.4$ (see the main text).

still visible in Eq. (4.5) as a small systematic deviation of θ from its theoretical value. Furthermore, Eq. (2.17) displays only the *leading* singular behavior of the correlation function in the KPZ universality class. For the ballistic deposition model studied here corrections to scaling not captured by Eq. (2.17) may lead to sizable numerical deviations. Therefore, the exponent θ measured here should be interpreted as an effective exponent. However, the numerical data for $C_L(0,t,t')$ follow a simple power law governed by this effective exponent quite accurately. Deviations from this power law begin to show only for $t'/t>0.4$, where one is clearly outside the short-time limit, and for $t'/t<0.03$, where microscopic aggregation effects come into play.

In $d=2$ the ballistic deposition model described here can be used to estimate the dynamic exponent z of the KPZ equation. The growth rule for ballistic deposition on a two-dimensional square lattice with $L\times L$ lattice sites is the natural extension of Eq. (4.2):

$$h_{j,k}(n+1)=\max[h_{j-1,k}(n),h_{j,k-1}(n),h_{j,k}(n)+1,$$
$$h_{j+1,k}(n),h_{j,k+1}(n)], \tag{4.6}$$

where periodic boundary conditions have been assumed. The lattice momentum has two components and is given by $\mathbf{q}=(2\pi/L)(m_1,m_2)$, where m_1 and m_2 are integers with $0\leq m_1,\ m_2\leq L-1$. The correlation function $C_L(\mathbf{q},t,t')$ is defined as in Eq. (4.4), where the lattice Fourier transform $\hat{h}_{\mathbf{q}}(n)$ of the deposition field is defined in analogy with Eq. (4.3). Note that $n=FL^2t$ with F normalized to unity relates n and t in this case so that t is again given by the number of layers deposited on the substrate. The short-time exponent θ can be measured as described above by measuring $C_L(\mathbf{q}=\mathbf{0},t,t')$ [see Eq. (4.4)] for $t'\ll t$. In order to keep the amount of CPU time needed for the simulation within reasonable limits we reduce t to $t=1000$ and take averages over 2×10^4 realizations of the deposition process. It turns out that a linear lattice size of $L=120$ sites is already sufficient to uniquely identify at least one decade for the scaling variable t'/t in which $C_L(\mathbf{0},t,t')$ obeys the simple power law predicted by Eq. (2.17). The overall behavior of $C_L(\mathbf{0},t,t')$ for $L \geqslant 120$ is qualitatively the same as displayed in Fig. 1, so that we refrain from reproducing it here. For $L=240$ and $0.01 \leqslant t'/t \leqslant 0.1$ we obtain

$$\theta = 1.655 \pm 0.052 \tag{4.7}$$

from a least-squares fit as the best estimate for θ from the available data. Using Eq. (2.18) we obtain the estimate

$$z = 1.642 \pm 0.052 \tag{4.8}$$

from Eq. (4.7) as our estimate for the dynamical exponent z in the KPZ universality class in $d=2$. A corresponding estimate for z can be obtained for $L=120$, which differs by less than half a standard deviation from the value given by Eq. (4.8), so that finite-size effects can be neglected within the statistical error. Finally, we note that according to Eqs. (1.7) and (4.8) one has $\alpha = 0.358 \pm 0.052$ for the roughness exponent. These values are in agreement with other numerical data for z and α in $d=2$ (see Chap. 8 of Ref. [1] for a collection of recent estimates) and they therefore provide some support for the general validity of Eqs. (2.10) and (2.18).

V. SUMMARY AND DISCUSSION

The following main results have been obtained.

(i) The short-time dynamics of the KPZ equation can be analyzed in close analogy to the short-time behavior of model A in critical relaxation. Starting from the operator identity given by Eq. (2.10), the analogy can be summarized as follows:

$$\frac{\partial}{\partial t} h(\mathbf{q},0) = 2D\tilde{h}(\mathbf{q},0) \Rightarrow Z_0 Z = Z_D^{-2} \tilde{Z}_0 \tilde{Z}; \tag{5.1a}$$

$$Z_D = (\tilde{Z}/Z)^{1/2}, \quad Z_0 = \tilde{Z}_0 \neq 1$$

for model A; and

$$Z = \tilde{Z} = 1, \quad \tilde{Z}_0 = 1, \quad Z_0 = Z_D^{-2} \tag{5.1b}$$

for the KPZ equation. In contrast to model A, the anomalous short-time scaling dimension θ of the deposition field h is given by the dynamical exponent z [see Eq. (2.18)], whereas the response field $\tilde{h}$ does not exhibit an anomalous short-time scaling dimension. The capability of analytical methods with regard to a full quantitative description of the crossover behavior from short to long times for the KPZ equation is limited. A perturbative analysis combined with dimensional considerations indicate that $\mathbf{q}^2(t-t')^2/t^{d/2}$ is the scaling argument that governs the leading finite-time corrections to the asymptotic long-time scaling behavior of the response function $G(\mathbf{q},t,t')$ in $d=1$. In the correlation function $C(\mathbf{q}=\mathbf{0},t,t')$ finite-time corrections persist indefinitely. A quantitative description of the full scaling behavior can probably be obtained by combining perturbative methods with mode coupling theory [10].

(ii) The short-time dynamics of ideal MBE according to Eq. (1.9) can be analyzed in close analogy to the short-time behavior of model B in critical relaxation. Starting again from Eq. (2.10), neither the deposition field h nor the response field $\tilde{h}$ exhibits anomalous short-time scaling dimensions, which is the same behavior as observed for model B [17]. In contrast to the KPZ equation, the infrared stable renormalization-group fixed point is *finite* in any dimension of physical interest. Therefore purely perturbative methods can be used to investigate the short-time to long-time crossover behavior of the response and the correlation function within, e.g., an $\varepsilon = d-4$ expansion. In combination with dimensional arguments, the perturbative analysis indicates that the scaling argument $q^4(t-t')^2/t^{d/4}$ governs the leading finite-time correction to the asymptotic long-time behavior of the response function $G(\mathbf{q},t,t')$. In the correlation function $C(\mathbf{q}=\mathbf{0},t,t')$ finite-time corrections again persist indefinitely.

(iii) With a simple ballistic deposition model Eq. (2.18) can be used to measure the dynamical exponent z for the KPZ universality class from a simulation of the short-time behavior of the height-height correlation function. Although such a simulation in principle requires short computer times, the overall benefit is somewhat limited due to the small signal-to-noise ratio in the correlations for $t' \ll t$ (see Fig. 1), which in turn must be compensated for by running the simulation with high statistics. In $d=1$, where Eq. (1.8) gives the exact scaling exponents, the numerical results for θ agree very well with the theoretical value $\theta = 4/3$, which is equivalent to $z=3/2$. In $d=2$ Eq. (2.18) has been successfully used to obtain a numerical estimate for the dynamical exponent z in the KPZ universality class [see Eq. (4.8)].

Finally, it should be mentioned that the short-time scaling behavior of the magnetization in an Ising model with model A (Glauber) dynamics can be efficiently used to determine the dynamic and static critical exponents in the Ising universality class [23]. It would be interesting to see to what extent Monte Carlo methods similar to those described here and in Ref. [23] can be used to study the asymptotic long-time scaling behavior of interfacial growth models from their short-time dynamics. The scaling relation between θ and z may also open an alternative path for direct numerical investigations of the KPZ equation.

ACKNOWLEDGMENTS

The author gratefully acknowledges useful correspondence with S. Pal, J. Krug, H.W. Diehl, and D.P. Landau.

APPENDIX A: GAUSSIAN THEORY

The Gaussian part $\mathcal{J}_0$ of the dynamic functional for Eq. (1.5) is the same as for model A of critical relaxation [17] and can be written in the symmetric form

$$\mathcal{J}_0[\tilde{h},h] = \frac{1}{2}\int \frac{d^dq}{(2\pi)^d}\int_0^\infty dt[\tilde{h}(-\mathbf{q},t),h(-\mathbf{q},t)]\mathcal{A}\begin{pmatrix}\tilde{h}(\mathbf{q},t)\\ h(\mathbf{q},t)\end{pmatrix}, \tag{A1}$$

where $h(\mathbf{q},0)=0$ and the response field fulfills the additional condition $\tilde{h}(\mathbf{q},\infty)=0$. The self-adjoint matrix operator $\mathcal{A}$ is then given by

$$\mathcal{A}=\begin{pmatrix} 2D & -\frac{\partial}{\partial t}-\nu\mathbf{q}^2 \\ \frac{\partial}{\partial t}-\nu\mathbf{q}^2 & 0 \end{pmatrix}. \tag{A2}$$

In terms of the source fields $\tilde{j}$ and j introduced by adding the source term

$$\mathcal{J}_j[\tilde{h},h]=\int\frac{d^dq}{(2\pi)^d}\int_0^\infty dt[\tilde{h}(\mathbf{q},t)\tilde{j}(-\mathbf{q},t)+h(\mathbf{q},t)j(-\mathbf{q},t)] \tag{A3}$$

to Eq. (A1), the generating functional

$$\mathcal{W}_0[\tilde{j},j]=\ln\int\mathcal{D}\tilde{h}\int\mathcal{D}h\exp\{\mathcal{J}_0[\tilde{h},h]+\mathcal{J}_j[\tilde{h},h]\} \tag{A4}$$

is conveniently evaluated by solving the set of initial value problems given by

$$2D\tilde{h}(\mathbf{q},t)-\left(\frac{\partial}{\partial t}+\nu\mathbf{q}^2\right)h(\mathbf{q},t)+\tilde{j}(\mathbf{q},t)=0,\quad h(\mathbf{q},t)=0$$

$$\left(\frac{\partial}{\partial t}-\nu\mathbf{q}^2\right)\tilde{h}(\mathbf{q},t)+j(\mathbf{q},t)=0,\quad \tilde{h}(\mathbf{q},\infty)=0 \tag{A5}$$

for $\tilde{h}$ and h. The more general initial condition $h(\mathbf{q},0)=h_0(\mathbf{q})$ can be incorporated in the source field $\tilde{j}(\mathbf{q},t)$ by the replacement

$$\tilde{j}(\mathbf{q},t)\rightarrow\tilde{j}(\mathbf{q},t)+\delta(t)h_0(\mathbf{q}). \tag{A6}$$

The solution of Eq. (A5), which is equivalent to calculating the inverse of the operator $\mathcal{A}$ [see Eq. (A2)], is given by

$$\begin{pmatrix}\tilde{h}(\mathbf{q},t)\\ h(\mathbf{q},t)\end{pmatrix}=\int_0^\infty dt'\begin{pmatrix}0 & G_0(\mathbf{q},t',t)\\ G_0(\mathbf{q},t,t') & C_0(\mathbf{q},t,t')\end{pmatrix}\begin{pmatrix}\tilde{j}(\mathbf{q},t')\\ j(\mathbf{q},t')\end{pmatrix}, \tag{A7}$$

where

$$G_0(\mathbf{q},t,t')=\Theta(t-t')e^{-\nu\mathbf{q}^2(t-t')},$$

$$C_0(\mathbf{q},t,t')=\frac{D}{\nu\mathbf{q}^2}(e^{-\nu\mathbf{q}^2|t-t'|}-e^{-\nu\mathbf{q}^2(t+t')}) \tag{A8}$$

are the response and correlation functions of Gaussian theory for the KPZ equation, respectively. From Eqs. (A4) and (A8) one obtains for the generating functional

$$\mathcal{W}_0[\tilde{j},j]=\int\frac{d^dq}{(2\pi)^d}\int_0^\infty dt\int_0^\infty dt'[j(-\mathbf{q},t)G_0(\mathbf{q},t,t')\tilde{j}(\mathbf{q},t')+\tfrac{1}{2}j(-\mathbf{q},t)C_0(\mathbf{q},t,t')j(\mathbf{q},t')]. \tag{A9}$$

For the general initial condition $h(\mathbf{q},0)=h_0(\mathbf{q})$ the corresponding generating functional is obtained by applying the replacement Eq. (A6) directly to Eq. (A9). The response and correlation propagators can now be obtained by functional derivatives of Eq. (A9) with respect to $\tilde{j}$ and j:

$$\mathcal{G}_0(\mathbf{q},t;\mathbf{q}',t')\equiv\langle h(\mathbf{q},t)\tilde{h}(\mathbf{q}',t')\rangle_0=(2\pi)^d\delta(\mathbf{q}+\mathbf{q}')G_0(\mathbf{q},t,t'),$$

$$\mathcal{C}_0(\mathbf{q},t;\mathbf{q}',t')\equiv\langle h(\mathbf{q},t)h(\mathbf{q}',t')\rangle_0=(2\pi)^d\delta(\mathbf{q}+\mathbf{q}')C_0(\mathbf{q},t,t'), \tag{A10}$$

where $\langle\ \rangle_0$ denote the average with respect to the Gaussian distribution generated by Eq. (A1). From momentum conservation it is obvious that the *full* two-point correlation functions $\mathcal{G}(\mathbf{q},t;\mathbf{q}',t')$ and $\mathcal{C}(\mathbf{q},t;\mathbf{q}',t')$ can be written in the same form as their Gaussian counterparts [see Eq. (A10)], which serves as the definition of the full response function $G(\mathbf{q},t,t')$ and the full correlation function $C(\mathbf{q},t,t')$. One should also note that the simultaneous requirements $h(\mathbf{q},0)=0$ and $\tilde{h}(\mathbf{q},\infty)=0$ forbid a Fourier transformation with respect to time so that one has to stick to the above mixed representation of the propagators for further calculations. Especially the normalization conditions imposed on correlation functions in order to define *renormalized* quantities [see Eqs. (2.6) and (2.7)] have to be reformulated accordingly. Note that the exponents α and z implied by Eq. (A8) are the Edwards-Wilkinson exponents given by Eq. (1.4).

In close analogy to the considerations described above, the Gaussian part of the dynamic functional for Eq. (1.9) is the same as for model B of critical relaxation [17,19] and can be written in the same symmetric form as given by Eq. (A1) together with the conditions $h(\mathbf{q},0)=0$ and $\tilde{h}(\mathbf{q},\infty)=0$. In this case the self-adjoint matrix operator $\mathcal{A}$ is given by

$$\mathcal{A}=\begin{pmatrix} 2D & -\frac{\partial}{\partial t}-\nu_1 q^4 \\ \frac{\partial}{\partial t}-\nu_1 q^4 & 0 \end{pmatrix}, \tag{A11}$$

where $q=|\mathbf{q}|$ is the modulus of the momentum vector $\mathbf{q}$. The generating functional given by Eq. (A4) is evaluated by solving the corresponding initial value problem for $\tilde{h}(\mathbf{q},t)$ and $h(\mathbf{q},t)$ [see Eq. (A5)]. The solution can be written in the same form as Eq. (A7), where instead of Eq. (A8) one has

$$G_0(\mathbf{q},t,t')=\Theta(t-t')e^{-\nu_1q^4(t-t')},$$

$$C_0(\mathbf{q},t,t')=\frac{D}{\nu_1q^4}(e^{-\nu_1q^4|t-t'|}-e^{-\nu_1q^4(t+t')}) \tag{A12}$$

for the response and the correlation function, respectively, of Gaussian theory for Eq. (1.9). With G_0 and C_0 taken from Eq. (A12), the corresponding response and correlation propa-

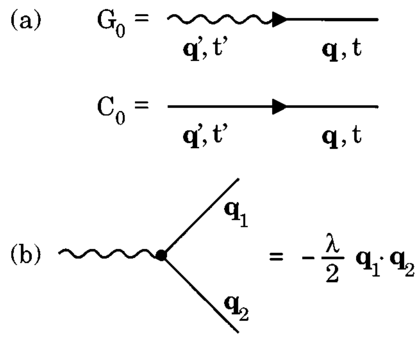

FIG. 2. (a) Graphical representation of the response propagator $\mathcal{G}_0$ and the correlation propagator $\mathcal{C}_0$ [see Eq. (A10)]. (b) Graphical representation of the vertex of Eq. (1.5) [see Eq. (2.2)]. The wiggly lines represent the response field $\tilde{h}(\mathbf{q},t)$ and the straight lines represent the deposition field $h(\mathbf{q},t)$.

gators are again given by Eq. (A10). We close this section by noting that the exponents α and z implied by Eq. (A12) are given by

$$z=4, \quad \alpha=(4-d)/2 \tag{A13}$$

in contrast to Eq. (1.11).

APPENDIX B: PERTURBATION THEORY

Due to the presence of strong-coupling fixed points in the KPZ equation, for $d\geqslant 2$ perturbation theory is only of limited value as compared to perturbation theory for model A critical dynamics, for example. However, some rigorous relations can be proved by analyzing the building blocks of perturbation theory for response and correlation functions and therefore some details concerning perturbative calculations for Eqs. (1.5) and (1.9) will be described below.

For the response and correlation propagators given by Eq. (A10) we use the graphical representation shown in Fig. 2(a). The vertex and its analytical expression can be read off from Eq. (2.2); they are shown in Fig. 2(b). The momentum carried by the response field in Fig. 2(b) is $-\mathbf{q}_1-\mathbf{q}_2$. Contributions to response, correlation, and vertex functions can be constructed from the elements in Fig. 2 according to the standard Feynman rules of dynamic perturbation theory [9,17,19]. As a first example we analyze the response function $G(\mathbf{q},t,t')$. Any contribution to G from a perturbation expansion can be cast into the form of the block diagram shown in Fig. 3. According to the Feyman rules, the first vertex contribution to an arbitrary diagram for G has to be arranged as shown in Fig. 3. The remainder of the diagram,

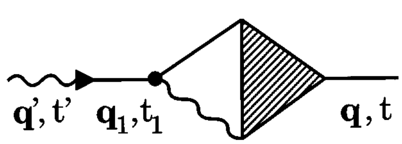

FIG. 3. Block diagram for the response function $G(\mathbf{q},t,t')$. The shaded triangle consists of an arbitrary number of vertices and propagators. To lowest order it is given by the vertex displayed in Fig. 2(b) (see the main text).

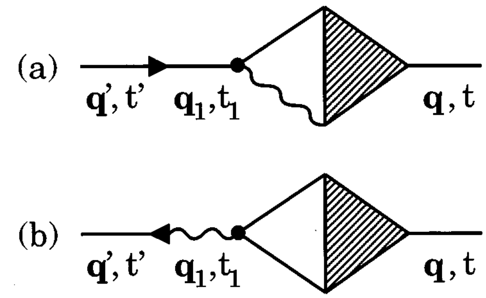

FIG. 4. Block diagrams for the correlation function $C(\mathbf{q},t,t')$. (a) Incoming correlation propagator $\mathcal{C}_0(\mathbf{q}_1,t_1;\mathbf{q}',t')$. (b) Incoming response propagator $\mathcal{G}_0(\mathbf{q}',t';\mathbf{q}_1,t_1)$ [see Eq. (A10) and the main text]. The shaded triangle has the same meaning as in Fig. 3.

which is not neccessarily one-particle irreducible, is indicated by the shaded triangle and may be interpreted as an arbitrary contribution to the three-point vertex function. To lowest order this three-point vertex function is shown in Fig. 2(b). From the explicit momentum dependence of the vertex it is obvious that for zero momentum $\mathbf{q}'=\mathbf{q}$ the block diagram displayed in Fig. 3 vanishes identically. One therefore finds the exact relation

$$G(\mathbf{q}=\mathbf{0},t,t')=G_0(\mathbf{q}=\mathbf{0},t,t')=\Theta(t-t') \tag{B1}$$

for the response function of Eq. (1.5).

In contrast to Fig. 3, the perturbative contributions to the correlation function $C(\mathbf{q},t,t')$ cannot be represented by a single block diagram. Instead, two types of block diagrams are required, as shown in Fig. 4. Due to the initial condition $h(\mathbf{q},0)=0$ both block diagrams vanish identically for $t'=0$. Following Ref. [17], Fig. 4 is used to obtain an exact expression for the *derivative* of C with respect to the time argument t'. The diagrams for $\partial C/\partial t'$ are of the same form as those for C. The main difference between the diagrams shown in Figs. 4(a) and 4(b) is that in Fig. 4(b) the internal time t_1 is restricted to the interval $0\leqslant t_1\leqslant t'$ due to causality, so that this block diagram vanishes identically for $t'=0$. The remaining block diagram [Fig. 4(a)] is of the same type as the block diagram for the response function G shown in Fig. 3. One therefore has a *termwise* correspondence between the perturbation series for $\partial C(\mathbf{q},t,t')/\partial t'|_{t'=0}$ and $G(\mathbf{q},t,t'=0)$. Gaussian theory [see Eq. (A8)] yields

$$\frac{\partial}{\partial t'}C_0(\mathbf{q},t,t'=0)=2De^{-\nu\mathbf{q}^2t}=2DG_0(\mathbf{q},t,t'=0) \tag{B2}$$

and Figs. 3 and 4(a) then show that the two perturbation series only differ by an overall factor $2D$. Therefore Eq. (B2) implies the relation

$$\frac{\partial}{\partial t'}C(\mathbf{q},t,t'=0)=2DG(\mathbf{q},t,t'=0) \tag{B3}$$

between the correlation function C and the reponse function G of the KPZ equation order by order in perturbation theory. According to the standard Feynman rules, the arguments presented above for C and G also hold for arbitrary n-point correlation functions that differ only in the propagator (response or correlation) assigned to one of the external legs. Therefore Eq. (B3) already establishes the proof of the operator identity Eq. (2.10) used in Sec. II. However, it must be pointed out here that the above arguments only constitute a rigorous proof of Eq. (B3) and therefore of Eq. (2.10) if the renomalization-group fixed point is accessible by perturbation theory. For the KPZ equation this is only possible in $d=1$. In $d \geqslant 2$ one encounters the well-known strong-coupling behavior that forms a formidable obstacle for analytic theories of dynamic scaling of Eq. (1.5) [9,10]. For the above derivation this means that Eq. (B3) may not hold in $d \geqslant 2$ at the renormalization-group fixed point despite its validity to all orders in perturbation theory. Nonetheless, the above perturbative analysis provides some evidence that Eq. (B3), and therefore Eq. (2.10), holds beyond $d=1$.

For Eq. (1.9) the building blocks of the perturbation theory can again be taken from Fig. 2, with the modification that the response and the correlation propagator [see Eq. (A10)] are now given by Eq. (A12) and that the expression $\lambda_1 \mathbf{q}_1 \cdot \mathbf{q}_2 (\mathbf{q}_1 + \mathbf{q}_2)^2$ must be assigned to each vertex as can be read off from Eq. (3.2). It is then straightforward to see that the arguments given above for the KPZ equation can be directly applied to ideal MBE dynamics, where no strong-coupling behavior is encountered in any spatial dimension of physical interest. The exact relations given by Eqs. (B1) and (B3) and the operator identity Eq. (2.10) therefore also hold for Eq. (1.9).

APPENDIX C: RESPONSE AND CORRELATION FUNCTIONS

In order to justify Eqs. (2.7) and (3.6) within the dimensional regularization scheme [9] in the $\mathbf{q},t$ representation and to obtain some indication how the short-time to long-time crossover takes place the response and correlation functions of Eqs. (1.5) and (1.9) are calculated here to one-loop order. The one-loop contribution to the response function for the KPZ equation is given by the block diagram shown in Fig. 3, where the shaded triangle is replaced by a single vertex shown in Fig. 2. The analytic expression for this diagram is then given by

$$G_1(\mathbf{q},t,t') = \lambda^2 \int_0^\infty dt_1 \int_0^\infty dt_2 \int \frac{d^d q'}{(2\pi)^d} (\mathbf{q}' \cdot \mathbf{q}) [\mathbf{q}' \cdot (\mathbf{q}' - \mathbf{q})] \times G_0(\mathbf{q},t_1,t') G_0(\mathbf{q}' - \mathbf{q},t_2,t_1) \times C_0(\mathbf{q}',t_2,t_1) G_0(\mathbf{q},t,t_2), \tag{C1}$$

where G_0 and C_0 are given by Eq. (A8). For simplicity we consider only Eq. (C1) in the limit $\mathbf{q} \to \mathbf{0}$, so that we can employ the expansion

$$G_0(\mathbf{q}' - \mathbf{q},t_2,t_1) = G_0(\mathbf{q}',t_2,t_1) \times [1 + 2\nu(\mathbf{q}' \cdot \mathbf{q})(t_2 - t_1) + O(\mathbf{q}^2)]. \tag{C2}$$

The $\mathbf{q}'$ integration in Eq. (C1) to leading order in $\mathbf{q}$ is then reduced to the calculation of second moments of a Gaussian in d dimensions. The result is

$$G_1(\mathbf{q},t,t') = \mathbf{q}^2 \frac{g}{2^d \pi^{d/2}} G_0(\mathbf{q},t,t') \times (2\nu)^{2-d/2} \int_{t'}^{t} dt_2 \int_{t'}^{t_2} dt_1 \left[\frac{d-2}{2d} (t_2 - t_1)^{-d/2} - \left(\frac{d-2}{2d} - \frac{t_1}{2t_2} \right) t_2^{-d/2} \right], \tag{C3}$$

where the effective coupling constant g is defined by Eq. (2.5). The remaining integrals in Eq. (C3) can be easily performed using dimensional regularization [9] with $d=2+\varepsilon$ in the exponents of $t_2 - t_1$ and t_2. Note that the prefactor $d-2$ in Eq. (C3) comes from an angular integration and must not be canceled by factors $1/\varepsilon$ indicating UV singularities in the time integral [9]. With the definition of u according to Eq. (2.6) ($Z_g = 1$ at this order) one obtains for $G(\mathbf{q},t,t') = G_0(\mathbf{q},t,t') + G_1(\mathbf{q},t,t')$

$$G(\mathbf{q},t,t') = G_0(\mathbf{q},t,t') \left\{ 1 - \frac{\mathbf{q}^2}{2} u \mu^{-\varepsilon} \left[\frac{d-2}{d\varepsilon} [2\nu(t-t')]^{2-d/2} + \frac{d-4}{4d} \frac{[2\nu(t-t')]^2}{(2\nu t)^{d/2}} \right] \right\}. \tag{C4}$$

The $1/\varepsilon$ pole (the UV singularity) in Eq. (C4) can be removed, e.g., by requiring $G(\mathbf{q},t^R,0)$ to stay finite for $\varepsilon \to 0$, where $t^R \equiv 1/(2\mu^2 \nu^R)$ is a reference time and ν^R is given by Eq. (2.6). Minimal subtraction yields the renormalization factor Z_ν quoted in Eq. (2.7). Note that the short-time contribution to G does not produce an additional $1/\varepsilon$ pole. By naively exponentiating the $\mathbf{q}$ dependence of G in the long-time limit one obtains at the infrared stable fixed point $u = u^* \neq 0$,

$$G^R(\mathbf{q},t,t') = \Theta(t-t') \exp\left[-\frac{\mathbf{q}^2}{2\mu^2} [2\nu^R \mu^2 (t-t')]^{2/z} \right] \times \left[1 - u^* \frac{\mathbf{q}^2}{\mu^2} \frac{d-4}{8d} \frac{[2\nu^R \mu^2 (t-t')]^2}{(2\nu^R \mu^2 t)^{d/2}} \right]. \tag{C5}$$

The predictive value of Eq. (C5) is very limited because u^* is *infinite* for $d \geqslant 2$. In $d=1$ Eq. (C5) indicates that the combination $(t-t')^2/t^{d/2}$ of the time arguments governs the crossover to the long-time scaling behavior of G for $t \to \infty$ with *fixed* $t-t'$. From dimensional arguments and the fact that the short-time contribution to G does not produce additional UV singularities we can infer that, according to Eq. (C5), $\mathbf{q}^2 (t-t')^2/t^{d/2}$ for $d=1$ is the scaling argument that governs the leading finite-time correction to the asymptotic long-time behavior of G. Furthermore, Eq. (C5) shows that G^R is analytic in t' for $t' \ll t$ at the one-loop level, but this behavior may be modified in higher orders. Finally, we note that the scaling form of the asymptotic long-time contribution to $G^R(\mathbf{q},t,t')$ given by the exponential in Eq. (C5) has recently been derived by combining perturbative methods with a mode coupling theory for the KPZ equation [10].

The correlation function $C(\mathbf{q},t,t')$ for Eq. (1.5) can be discussed in much the same way as the response function. This time we simplify the calculations even further by limiting ourselves to $\mathbf{q}=\mathbf{0}$. In this case only the diagram in Fig. 4(b) contributes and we obtain to one-loop order

$$C(\mathbf{0},t,t')=2D\min(t,t') + \frac{\lambda^2}{2}\int_0^t dt_2 \int_0^{t'} dt_1 \int \frac{d^dq}{(2\pi)^d} q^4 [C_0(\mathbf{q},t_1,t_2)]^2, \tag{C6}$$

where C_0 is given by Eq. (A8). The integrations in Eq. (C6) can be easily performed and using dimensional regularization one arrives at

$$\begin{aligned} C(\mathbf{0},t,t'\leq t)=2D\bigg(t' + \frac{u\mu^{-\varepsilon}}{4\nu\varepsilon}\{[2\nu(t-t')]^{2-d/2} \\ -[2\nu(t+t')]^{2-d/2}+(2\nu t)^{2-d/2} \\ \times[(4-d)(t'/t)-d(t'/t)^{2-d/2}]\}\bigg), \end{aligned} \tag{C7}$$

where Eq. (2.6) has been used with $Z_g=1$. The $1/\varepsilon$ pole in Eq. (C7) can be removed by demanding that $C(\mathbf{0},t^R,t^R)$ is finite, where $t^R \equiv 1/(4\mu^2\nu^R)$ is chosen as the reference time. Using minimal subtraction one finds the renormalization factor Z_D quoted in Eq. (2.7). For $t' \ll t$ Eq. (C7) can be simplified to

$$C(\mathbf{0},t,t'\ll t)=2Dt'\left[1-\frac{u}{\varepsilon}\frac{d}{2}(2\nu\mu^2 t')^{1-d/2}+O(t'^2)\right], \tag{C8}$$

which explicitly shows that the short-time contribution to C produces an additional $1/\varepsilon$ pole. For $t'>0$ the renormalized correlation function can be naively exponentiated at the infrared stable fixed point $u=u^*\neq 0$. The result is

$$\begin{aligned} C^R(\mathbf{0},t,t'\leq t)=D^R\{(t+t')[2\nu^R\mu^2(t+t')]^{\theta-1}-(t-t') \\ \times[2\nu^R\mu^2(t-t')]^{\theta-1}-2\theta t'(2\nu^R\mu^2 t)^{\theta-1} \\ +2t'(2\nu^R\mu^2 t')^{\theta-1}\}, \end{aligned} \tag{C9}$$

where θ is the short-time exponent given by Eq. (2.18) and $d=1$ has been assumed. The short-time scaling behavior for $t' \ll t$ is also reproduced by Eq. (C9). However, from Eqs. (2.10) and (B1) one expects $(\partial/\partial t')C^R(\mathbf{0},t,t'=0)=2D^R$, which is *not* reproduced by Eq. (C9), because $\theta>1$. Therefore Eq. (C9) can give only a rough idea of the true scaling form of the correlation function C^R for the KPZ equation. However, Eq. (C9) indicates that for $\mathbf{q}=\mathbf{0}$ short-time corrections to the correlation function persist indefinitly [see also Eq. (C7)].

For ideal MBE dynamics according to Eq. (1.9), the one-loop contribution to the response function is again given by the block diagram shown in Fig. 3, where the shaded triangle is replaced by a single vertex. The analytic expression for this diagram is then given by

$$\begin{aligned} G_1(\mathbf{q},t,t')=4\lambda_1^2\mathbf{q}^2\int_0^\infty dt_1\int_0^\infty dt_2\int \frac{d^dq'}{(2\pi)^d}(\mathbf{q}'\cdot\mathbf{q}) \\ \times[\mathbf{q}'\cdot(\mathbf{q}'-\mathbf{q})](\mathbf{q}'-\mathbf{q})^2 G_0(\mathbf{q},t_1,t') \\ \times G_0(\mathbf{q}'-\mathbf{q},t_2,t_1)C_0(\mathbf{q}',t_2,t_1)G_0(\mathbf{q},t,t_2), \end{aligned} \tag{C10}$$

where G_0 and C_0 are given by Eq. (A12). For simplicity, we consider only Eq. (C10) in the limit $\mathbf{q}\to\mathbf{0}$, i.e., we use the expansion

$$\begin{aligned} G_0(\mathbf{q}'-\mathbf{q},t_2,t_1)=G_0(\mathbf{q}',t_2,t_1) \\ \times[1+4\nu_1\mathbf{q}'^2(\mathbf{q}'\cdot\mathbf{q})(t_2-t_1)+O(\mathbf{q}^2)]. \end{aligned} \tag{C11}$$

The $\mathbf{q}'$ integration in Eq. (C10) to leading order in $\mathbf{q}$ yields

$$\begin{aligned} G_1(\mathbf{q},t,t')=\frac{q^4}{4}\frac{g_1}{2^d\pi^{d/2}}\frac{\Gamma(d/4)}{\Gamma(d/2)}G_0(\mathbf{q},t,t')(2\nu_1)^{2-d/4} \\ \times\int_{t'}^t dt_2\int_{t'}^{t_2}dt_1\bigg[\frac{d-6}{d}(t_2-t_1)^{-d/4} \\ -\left(\frac{d-6}{d}-\frac{t_1}{t_2}\right)t_2^{-d/4}\bigg], \end{aligned} \tag{C12}$$

where the effective coupling constant g_1 is defined by Eq. (3.4). As in Eq. (C3), the remaining integrals in Eq. (C12) can be performed using dimensional regularization with $d=4+\varepsilon$ in the exponents of t_2-t_1 and t_2. As usual, the $1/\varepsilon$ poles indicate UV singularities in the time integral. With the definition of u according to Eq. (3.5) and $Z_{g_1}=1$, one obtains for $G(\mathbf{q},t,t')=G_0(\mathbf{q},t,t')+G_1(\mathbf{q},t,t')$, in the limit $t\to\infty$ with $t-t'=$ const,

$$\begin{aligned} G(\mathbf{q},t,t')=G_0(\mathbf{q},t,t') \\ \times\bigg\{1-\frac{q^4}{2}u\mu^{-\varepsilon}\bigg[\frac{d-6}{d\varepsilon}[2\nu_1(t-t')]^{2-d/4} \\ +\frac{3}{4}\frac{d-8}{4d}\frac{[2\nu_1(t-t')]^2}{(2\nu_1 t)^{d/4}}\bigg]\bigg\} \end{aligned} \tag{C13}$$

up to terms $O((t-t')^3/t^{d/4+1})$. The $1/\varepsilon$ pole (the UV singularity) in Eq. (C13) can be removed by the minimal subtraction scheme described above, where $t^R\equiv 1/(2\mu^4\nu_1^R)$ defines the reference time and ν_1^R is given by Eq. (3.5). One obtains the renormalization factor Z_{ν_1} quoted in Eq. (3.6). By naively exponentiating the $\mathbf{q}$ dependence of G in the long-time limit one obtains, at the infrared stable fixed point $u=u^*\neq 0$,

$$\begin{aligned} G^R(\mathbf{q},t,t')=\Theta(t-t')\exp\left[-\frac{q^4}{2\mu^4}[2\nu_1^R\mu^4(t-t')]^{4/z}\right] \\ \times\left[1-\frac{3}{4}u^*\frac{q^4}{\mu^4}\frac{d-8}{8d}\frac{[2\nu_1^R\mu^4(t-t')]^2}{(2\nu_1^R\mu^4 t)^{d/4}}\right]. \end{aligned} \tag{C14}$$

In contrast to Eq. (1.5), the infrared stable fixed point for Eq. (1.9) is *finite* in any dimension of physical interest. In particular one has $u^* = O(\varepsilon)$, so that an ε expansion around the upper critical dimension $d_c = 4$ can be performed. The qualitative behavior of G^R according to Eq. (C14) is very similar to the behavior of G^R for the KPZ equation in $d=1$ [see Eq. (C5)]. Here the leading finite-time correction to the asymptotic long-time behavior is governed by the combination $(t-t')^2/t^{d/4}$ of time arguments.

The one-loop contribution to the correlation function $C(\mathbf{q}=\mathbf{0},t,t')$ for Eq. (1.9) vanishes identically due to an additional factor $\mathbf{q}^2$ in the vertex [see Eq. (C10)] so that

$$C^R(\mathbf{0},t,t') = 2D\min(t,t') + O(u^2). \tag{C15}$$

Equation (C15) directly demonstrates that $Z_D = 1$, as quoted in Eq. (3.6), to one-loop order. As in the case of KPZ dynamics, Eq. (C15) demonstrates that finite-time corrections to the correlation function for Eq. (1.9) persist indefinitely for $\mathbf{q}=\mathbf{0}$.

[1] A.-L. Barabasi and H.E. Stanley, *Fractal Concepts in Surface Growth* (Cambridge University Press, New York, 1995), and references therein.
[2] S. Das Sarma, C.J. Lanczycki, R. Kotlyar, and S.V. Ghaisas, Phys. Rev. E **53**, 359 (1996), and references therein.
[3] J. Krug and H. Spohn, Phys. Rev. A **38**, 4271 (1988); J. Krug, J. Phys A **22**, L769 (1989); J. Krug, M. Plischke, and M. Siegert, Phys. Rev. Lett. **70**, 3271 (1993).
[4] J. Krug, Phys. Rev. Lett. **72**, 2907 (1994).
[5] S. Pal and D.P. Landau, Phys. Rev. B **49**, 10 597 (1994), and references therein.
[6] J. Krim, I. Heyvaert, C. Van Haesendock, and Y. Bruynseraede, Phys. Rev. Lett. **70**, 57 (1993).
[7] S.F. Edwards and D.R. Wilkinson, Proc. R. Soc. London Ser. A **381**, 17 (1982).
[8] M. Kadar, G. Parisi, and Y.-C. Zhang, Phys. Rev. Lett. **56**, 889 (1986).
[9] E. Frey and U.C. Täuber, Phys. Rev. E **50**, 1024 (1994).
[10] E. Frey, U.C. Täuber, and T. Hwa, Phys. Rev. E **53**, 4424 (1996).
[11] U. Deker and F. Haake, Phys. Rev A **11**, 2043 (1975).
[12] K. Sneppen, J. Krug, M.H. Jensen, C. Jayaprakash, and T. Bohr, Phys. Rev. A **46**, R7351 (1992).
[13] Z.W. Lai and S. Das Sarma, Phys. Rev. Lett. **66**, 2348 (1991).
[14] S. Das Sarma and R. Kotlyar, Phys. Rev. E **50**, R4275 (1994).
[15] D. Wolf and J. Villain, Europhys. Lett. **13**, 389 (1990).
[16] T. Sun, H. Guo, and M. Grant, Phys. Rev. A **40**, 6763 (1989).
[17] H.K. Janssen, B. Schaub, and B. Schmittmann, Z. Phys. B **73**, 539 (1989).
[18] P.C. Martin, E.D. Siggia, and H.H. Rose, Phys. Rev. A **8**, 423 (1973).
[19] P.C. Hohenberg and B.I. Halperin, Rev. Mod. Phys. **49**, 435 (1977).
[20] M. Lässig, Nucl. Phys. B **448**, 559 (1995).
[21] H.W. Diehl, in *Phase Transitions and Critical Phenomena*, edited by C. Domb and J.L. Lebowitz (Academic, London, 1986), Vol. 10.
[22] J. Krug, Phys. Rev. A **44**, R801 (1991).
[23] Z.B. Li, L. Schülke, and B. Zheng, Phys. Rev. Lett. **74**, 3396 (1995).